

Silver Ions-Mediated Conformational Switch: Facile Design of Structure-Controllable Nucleic Acid Probes

Yongxiang Wang,^{†,‡} Jishan Li,[†] Hao Wang,^{†,‡} Jianyu Jin,^{†,‡} Jinhua Liu,[‡] Kemin Wang,[†] Weihong Tan,^{†,§} and Ronghua Yang^{*,†}

State Key Laboratory of Chemo/Biosensing and Chemometrics, College of Chemistry and Chemical Engineering, Hunan University, Changsha, 410082, Beijing National Laboratory for Molecular Sciences, College of Chemistry and Molecular Engineering, Peking University, Beijing, 100871, China, and Center for Research at the Bio/Nano Interface, Department of Chemistry and Department of Physiology and Functional Genomics, Shands Cancer Center and UF Genetics Institute, University of Florida, Gainesville, Florida 32611-7200

Conformationally constraint nucleic acid probes were usually designed by forming an intramolecular duplex based on Watson–Crick hydrogen bonds. The disadvantages of these approaches are the inflexibility and instability in complex environment of the Watson–Crick-based duplex. We report that this hydrogen bonding pattern can be replaced by metal-ligation between specific metal ions and the natural bases. To demonstrate the feasibility of this principle, two linear oligonucleotides and silver ions were examined as models for DNA hybridization assay and adenosine triphosphate detection. The both nucleic acids contain target binding sequences in the middle and cytosine (C)-rich sequences at the lateral portions. The strong interaction between Ag^+ ions and cytosines forms stable $\text{C–Ag}^+\text{–C}$ structures, which promises the oligonucleotides to form conformationally constraint formations. In the presence of its target, interaction between the loop sequences and the target unfolds the $\text{C–Ag}^+\text{–C}$ structures, and the corresponding probes unfolding can be detected by a change in their fluorescence emission. We discuss the thermodynamic and kinetic opportunities that are provided by using Ag^+ ion complexes instead of traditional Watson–Crick-based duplex. In particular, the intrinsic feature of the metal-ligation motif facilitates the design of functional nucleic acids probes by independently varying the concentration of Ag^+ ions in the medium.

Sensitive, selective, rapid, and cost-effective analysis of biomolecules, such as nucleic acid and proteins, is critically important in areas such as of clinical, environmental, and food safety applications.¹ To date, various analytical technologies, based on Raman scattering,^{2–7} electrochemical detection,^{8–11} colorim-

etry,^{12–14} photoluminescence,^{15–19} field effect transistor,²⁰ and chemoluminescence,²¹ have been developed for nucleic acids detections. Of which homogeneous hybridization assays with fluorescent DNA probes have been extensively used due to the inherent advantages, such as operation convenience, high sensitivity and potential compatibility.^{22–25} For this design, switching of DNA structure between different conformations is a subject of particular current interest. Such probes consist of fluorophore-quencher pairs, by forming an intramolecular duplex through

- (3) Bruchez, M.; Moronne, M.; Gin, P.; Weiss, S.; Alivisatos, A. P. *Science* **1998**, *281*, 2013–2016.
- (4) Chan, W. C. W.; Nie, S. M. *Science* **1998**, *281*, 2016–2018.
- (5) Cao, Y. C.; Jin, R. C.; Nam, J.-M.; Thaxton, C. S.; Mirkin, C. A. *J. Am. Chem. Soc.* **2003**, *125*, 14676–14677.
- (6) Patolsky, F.; Gill, R.; Weizmann, Y.; Mokari, T.; Banin, U.; Willner, I. *J. Am. Chem. Soc.* **2003**, *125*, 13918–13919.
- (7) Grubisha, D. S.; Lipert, R. J.; Park, H. Y.; Driskell, J.; Porter, M. D. *Anal. Chem.* **2003**, *75*, 5936–5943.
- (8) Xiao, Y.; Lou, X.; Uzawa, T.; Plakos, K. J. I.; Plaxco, K. W.; Soh, H. T. *J. Am. Chem. Soc.* **2009**, *131*, 15311–15316.
- (9) Jelen, F.; Olejniczak, A. B.; Kourilova, A.; Lesnikowski, Z. J.; Palecek, E. *Anal. Chem.* **2009**, *81*, 840–844.
- (10) Chen, C.-P.; Ganguly, A.; Wang, C.-H.; Hsu, C.-W.; Chattopadhyay, S.; Hsu, Y.-K.; Chang, Y.-C.; Chen, K.-H.; Chen, L.-C. *Anal. Chem.* **2009**, *81*, 36–42.
- (11) Tansil, N. C.; Xie, H.; Xie, F.; Gao, Z. *Anal. Chem.* **2005**, *77*, 126–134.
- (12) Elghanian, R.; Storhoff, J. J.; Mucic, R. C.; Letsinger, R. L.; Mirkin, C. A. *Science* **1997**, *277*, 1078–1081.
- (13) Alivisatos, P. *Nat. Biotechnol.* **2004**, *22*, 47–52.
- (14) Katz, E.; Willner, I. *Angew. Chem., Int. Ed.* **2004**, *43*, 6042–6108.
- (15) Mahtab, R.; Rogers, J. P.; Murphy, C. J. *J. Am. Chem. Soc.* **1995**, *117*, 9099–9100.
- (16) Mahtab, R.; Rogers, J. P.; Singleton, C. P.; Murphy, C. J. *J. Am. Chem. Soc.* **1996**, *118*, 7028–7032.
- (17) Mahtab, R.; Harden, H. H.; Murphy, C. J. *J. Am. Chem. Soc.* **2000**, *122*, 14–17.
- (18) Krasnoperov, L. N.; Marras, S. A. E.; Kozlov, M.; Wirpsza, L.; Mustaev, A. *Bioconjugate Chem.* **2010**, *21*, 319–327.
- (19) Jiang, G.; Susha, A. S.; Lutich, A. A.; Stefani, F. D.; Feldmann, J.; Rogach, A. L. *ACS Nano* **2009**, *3*, 4127–4131.
- (20) Uno, T.; Tabata, H.; Kawai, T. *Anal. Chem.* **2007**, *79*, 52–59.
- (21) Patolsky, F.; Weizmann, Y.; Katz, E.; Willner, I. *Angew. Chem., Int. Ed.* **2003**, *42*, 2372–2376.
- (22) Lakowicz, J. R. *Principles of Fluorescence Spectroscopy*, 3rd ed.; Springer: New York, 2006.
- (23) Yang, C. Y.; Medley, C. D.; Tan, W. H. *Curr. Pharm. Biotechnol.* **2005**, *6*, 445–452.
- (24) Algar, W. R.; Krull, U. J. *Anal. Chem.* **2009**, *81*, 4113–4120.
- (25) Willner, I.; Katz, E. *Angew. Chem., Int. Ed.* **2004**, *43*, 6042–6108.

* To whom correspondence should be addressed: Fax: +86-731-88822523. E-mail: Yangrh@pku.edu.cn.

[†] Hunan University.

[‡] Peking University.

[§] University of Florida.

(1) Liu, J. W.; Cao, Z. H.; Lu, Y. *Chem. Rev.* **2009**, *109*, 1948–1998.

(2) Li, Y. C.; Wang, Z.; Ou, L. M. L.; Yu, H.-Z. *Anal. Chem.* **2007**, *79*, 426–433.

Watson–Crick hydrogen bonds^{26,27} to ensure efficient Förster fluorescence resonance energy transfer (FRET), for which distance-dependent fluorescence quenching is elaborately designed to be closely associated with DNA hybridization events.^{28–30}

Although the hairpin-structured probes based on Watson–Crick hydrogen bonds have been widely used in broad areas, such as genetic screening biosensor development, biochip construction, the detection of single nucleotide polymorphisms (SNPs), and messenger-RNA (mRNA) monitoring in living cells,³¹ the instability in complex environment and inflexibility of the stem constructed by natural base pairs are the challenges for their applications. To meet this shortcoming, a triplex hairpin-shaped probe has been recently designed by Seitz et al. through introducing a DNA competitor in the stem portion.³² The DNA competitor hybridizes with the stem sequence to form a triplex-stem, but allows dehybridization when the loop sequences bind to its target molecule. Choice of different DNA competitor offers a general means for more precisely modulating stem stability and flexibility without resynthesis of the probe molecules.

The other strategy is using metal-ligation interaction. Metal ions may stabilize several of the non-Watson–Crick systems. The high specificity of interaction of oligonucleotides with metal ion makes the oligonucleotides the current tools for not only detections of metal ions,^{33–41} but also design of alternative approaches for detections of amino acids,⁴² DNA,^{43–45} or redox environments.⁴⁶ For instances, a G-quadruplex-based molecular beacon

(MB) has been recently developed by Gosse et al.⁴⁷ The intrinsic feature of the quadruplex motif facilitates the design of functional MBs by independently varying the concentration of K⁺ ions or Na⁺ ions in the medium. But the instability of quadruplex in complex environment makes it be difficult for applications such as real-time qPCR and measurements in vivo. More recently, two MBs based on the stable T-Hg²⁺-T base pairs were developed by Chang et al. and our group.^{44,45} Both the thermodynamic and kinetic features of the MBs could be conveniently modulated by independently varying the Hg²⁺ ions concentration. However, the slow DNA hybridization dynamics of the MBs and tremendous toxicity of Hg²⁺ ions restrict their application as universal biosensors. There is still need to search for other metal ions in these approaches that could improve the probe stability, speed the DNA hybridization dynamics, and avoid the use of toxic Hg²⁺ ions.

Silver ion (Ag⁺) has been employed as clinical material because of its antibacterial activity.⁴⁸ Interactions of Ag⁺ ions with nucleic acids have been studied extensively. It has been reported the selective interaction between mismatched cytosine (C) base pairs and Ag⁺ forms the strong and stable C–Ag⁺-C complex.^{49–51} Using DNA oligomer including tandem cytosine-cytosine mismatches, highly selective and sensitive Ag⁺ ions sensors have been developed.^{39–41} However, to the best of our knowledge, no attention has been given to designing functional nucleic acids probes using the C–Ag⁺-C structure. Compared to the uses of K⁺ and Hg²⁺ for this design, Ag⁺ would be a better candidate. Because the stability of C–Ag⁺-C is stronger than that of K⁺-G-quadruplex, but is weaker than that of T-Hg²⁺-T,⁵⁰ which is feasible to improve the DNA hybridization dynamics. Moreover, Ag⁺ ions have much lower toxicity than Hg²⁺ ions. Therefore, we expect that the preceding structures can be replaced by a C–Ag⁺-C motif to achieve an advanced biosensing approach. To demonstrate the feasibility of this motif, in the present work, we designed two conformationally constrained nucleic acid probes based on the intramolecular C–Ag⁺-C structures for DNA hybridization assay and adenosine triphosphate (ATP) detection. It is the Ag⁺ ions ligation interaction that allows tuning the stem stability of the probes, thereby achieving higher target-binding selectivity and sensitivity than conventionally structured DNA probes, such as MBs and MB-aptamers.^{52,53}

EXPERIMENTAL SECTION

Materials and Apparatus. All oligonucleotides were prepared by TaKaRa Biotechnology Co., Ltd., (Dalian, China). They were dissolved in sterilized Milli-Q ultrapure water (18.2 MΩ) as stock solutions and were kept at –4 °C. The oligonucleotides concentrations were accurately identified according to UV absorption at 260

- (26) Tyagi, S.; Kramer, F. R. *Nat. Biotechnol.* **1996**, *14*, 303–308.
- (27) Tyagi, S.; Marras, S. A. E.; Kramer, F. R. *Nat. Biotechnol.* **2000**, *18*, 1191–1196.
- (28) Marras, S. A. E.; Kramer, F. R.; Tyagi, S. *Nucleic Acids Res.* **2002**, *30*, e122.
- (29) Sassolas, A.; Leca-Bouvier, B. D.; Blum, L. J. *Chem. Rev.* **2008**, *108*, 109–139.
- (30) Zhang, P.; Beck, T.; Tan, W. H. *Angew. Chem., Int. Ed.* **2001**, *40*, 402–405.
- (31) Wang, K. M.; Tang, Z. W.; Yang, C. J.; Kim, Y.; Fang, X. H.; Li, W.; Wu, Y. R.; Medley, C. D.; Cao, Z. H.; Li, J.; Colon, P.; Lin, H.; Tan, W. H. *Angew. Chem., Int. Ed.* **2009**, *48*, 856–870.
- (32) Grossmann, T. N.; Röglin, L.; Seitz, O. *Angew. Chem., Int. Ed.* **2007**, *46*, 5223–5225.
- (33) Ueyama, H.; Takagi, M.; Takenaka, S. *J. Am. Chem. Soc.* **2002**, *124*, 14286–14287.
- (34) Nagatoishi, S.; Nojima, T.; Juskowiak, B.; Takenaka, S. *Angew. Chem., Int. Ed.* **2005**, *44*, 5067–5070.
- (35) He, F.; Tang, Y. L.; Wang, S.; Li, Y. L.; Zhu, D. B. *J. Am. Chem. Soc.* **2005**, *127*, 12343–12346.
- (36) Ono, A.; Togashi, H. *Angew. Chem., Int. Ed.* **2004**, *43*, 4300–4302.
- (37) Gao, X. Y.; Xing, G. M.; Yang, Y. L.; Shi, X. L.; Liu, R.; Chu, W. G.; Jing, L.; Zhao, F.; Ye, C.; Yuan, H.; Fang, X. H.; Wang, C.; Zhao, Y. L. *J. Am. Chem. Soc.* **2008**, *130*, 9190–9191.
- (38) Wang, H.; Wang, Y. X.; Jin, J. Y.; Yang, R. H. *Anal. Chem.* **2008**, *80*, 9021–9028.
- (39) Ono, A.; Cao, S.; Togashi, H.; Tashiro, M.; Fujimoto, T.; Machinami, T.; Oda, S.; Miyake, Y.; Okamoto, I.; Tanaka, Y. *Chem. Commun.* **2008**, 4825–4827.
- (40) Lin, Y.-H.; Tseng, W.-L. *Chem. Commun.* **2009**, 6619–6621.
- (41) Wen, Y. Q.; Xing, F. F.; He, S. J.; Song, S. P.; Wang, L. H.; Long, Y. T.; Li, D.; Fan, C. H. *Chem. Commun.* **2010**, 46, 2596–2598.
- (42) Lee, J. S.; Ulmann, P. A.; Han, M. S.; Mirkin, C. A. *Nano Lett.* **2008**, *8*, 529–533.
- (43) Wang, Y. X.; Li, J. S.; Jin, J. Y.; Wang, H.; Tang, H. X.; Yang, R. H.; Wang, K. M. *Anal. Chem.* **2009**, *81*, 9703–9709.
- (44) Lin, Y.-W.; Ho, H.-T.; Huang, C.-C.; Chang, H.-T. *Nucleic Acids Res.* **2008**, *36*, e123.
- (45) Yang, R. H.; Jin, J. Y.; Long, L. P.; Wang, Y. X.; Wang, H.; Tan, W. H. *Chem. Commun.* **2009**, 322–324.
- (46) Miyake, Y.; Ono, A. *Tetrahedron Lett.* **2005**, *46*, 2441–2443.

- (47) Bourdoncle, A.; Torres, A. E.; Gosse, C.; Lacroix, L.; Vekhoff, P.; LeSaux, T. L.; Jullien, L. J. *Am. Chem. Soc.* **2006**, *128*, 11094–11105.
- (48) Bhardwaj, V. K.; Singh, N.; Hundal, M. S.; Hundal, G. *Tetrahedron* **2006**, *62*, 7878–7886.
- (49) Dattagupta, N.; Crothers, D. M. *Nucleic Acids Res.* **1981**, *9*, 2971–2985.
- (50) Ono, A.; Miyake, Y. *Nucleic Acids Symp. Ser.* **2003**, *3*, 227–228.
- (51) Shukla, S.; Sastry, M. *Nanoscale* **2009**, *1*, 122–127.
- (52) Fang, X. H.; Li, J. J.; Perlette, J.; Tan, W. H.; Wang, K. M. *Anal. Chem.* **2000**, *72*, 747A–753A.
- (53) Hamaguchi, N.; Ellington, A.; Stanton, M. *Anal. Biochem.* **2001**, *294*, 126–131.

Table 1. Oligonucleotides Sequences Used in This Work^a

type	sequences
P ₁	5'-dabcy1-CCCCCAGAGAGGTAGTATGGTGTACCCCC-FAM-3'
P ₂	5'-dabcy1-CACCTGGGGAGTATTGCGGAGGAAGG(T) ₃₂ CACCTC-FAM-3'
P ₃	5'-CCCCCAGAGAGGTAGTATGGTGTACCCCC-FAM-3'
T _p	5'-TACACCATACTACCTCTCT-3'
T _{sm}	5'-TACACCATAATACCTCTCT-3'

^a T_p and T_{sm} represent the perfectly matched target DNA and single-base mismatched DNA, respectively.

nm. 3-[*N*-morpholino]propanesulfonic acid (MOPS) was provided by China National Medicines Co. Ltd. (Beijing, China). AgNO₃, NaNO₃, Mg(NO₃)₂, ATP, adenosine monophosphate (AMP), adenosine diphosphate (ADP), cytidine triphosphate (CTP), and guanosine triphosphate (GTP) used in this work were purchased from Aldrich (Milwaukee, WI, USA) without further purification. 0.1 M stock solution of AgNO₃ was prepared by dissolving desired amount of the material in Milli-Q ultrapure water. All work solutions were prepared with MOPS buffer solution (10 mM, pH 7.0, 100 mM NaNO₃, 2.5 mM Mg(NO₃)₂).

UV-visible absorption spectra were recorded on a Hitachi U-4100 UV-vis spectrophotometer (Kyoto, Japan). All fluorescence measurements were performed on a Hitachi F-7000 fluorescence spectrofluorometer (Kyoto, Japan). The pH was measured by a model 868 pH meter (Orion). Temperature was controlled by PolyScience 9112 refrigerating/heating circulators.

Interaction of Nucleic Acids with Ag⁺ Ions. For evaluation of the metal-induced fluorescence quenching of P₁, P₂ or P₃ (Table 1), 500 μL the nucleic acids aqueous solution (50 nM) was titrated with Ag⁺ ions by direct addition of small aliquots (typically 20 μL) of the metal stock solutions into the quartz cell with a micropipet. Fluorescence emission spectra were recorded immediately after fully mixing metal ion with the probe solution.

DNA Hybridization Assay. For DNA hybridization assay, 50 μL 0.5 μM of the capture DNA P₁, 100 μL 5.0 μM Ag⁺ ions, and 50 μL of the target DNA or blank buffer solution were mixed and diluted to 500 μL with MOPS buffer. After the stirring for ~1 min at room temperature, the fluorescence emission spectra were recorded.

To test the kinetic behaviors of DNA hybridization, fluorescence intensity of 500 μL of the MOPS buffer, containing 1.0 μM Ag⁺, 50 nM P₁, and a proper amount of perfectly cDNA target T_p (Table 1) was monitored at 512 nm with an excitation wavelength of 480 nm. The addition was limited to 25 μL so that the volume change was insignificant.

The thermo stability of the complexes of P₁ and Ag⁺ ions at different temperatures was explored. The fluorescence intensity at 518 nm was measured at every 5 centigrade ranging from 15 to 85 °C.

RESULTS AND DISCUSSION

Principle of Operation. To test the feasibility of this approach, two linear oligonucleotides were selected: P₁ for DNA hybridization assay, and P₂ for ATP detection. The both oligonucleotides contained C-rich Ag⁺-binding sequences at the lateral portions and were labeled with fluorescein (FAM) and 4-(4'-(dimethylamino) phenylazo) benzoic acid (dabcy1) to the 3'- and 5'-termini, respectively. To examine the effect of Ag⁺ on the FAM fluorescence quenching, an oligonucleotide (P₃) which con-

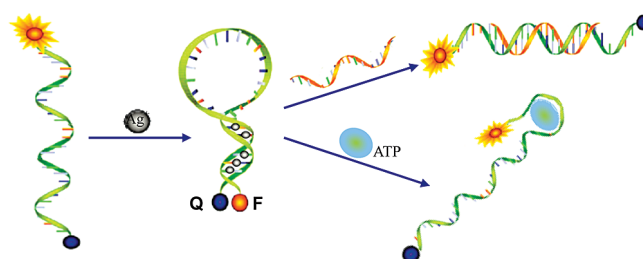


Figure 1. Schematic representation of the stem flexibility-controllable DNA probes for signaling molecular interactions. F and Q represent the fluorophore and quencher, respectively.

tained the same sequence as P₁ but was only labeled with FAM at the 3'-termini was chosen as a control. The target DNA molecules, T_p and T_{sm}, were 19-mer long and were either perfectly complementary to the bases of P₁ or contained one mismatch base with P₁, respectively. Figure 1 shows the operation principle for detection of DNA hybridization or ATP. In the absence of Ag⁺ ions, the oligonucleotide is normal single-stranded DNA sequences with random-coil structure, and emits strong FAM fluorescence. In the presence of Ag⁺ ions, the formation of C–Ag⁺–C structures facilitates the oligonucleotide to fold into a hairpin structure, the FAM fluorescence was thus quenched due to space proximity of the fluorophore and quencher. In the presence of a target molecule, interaction between the loop sequence of the oligonucleotide and the target destroyed the hairpin structure, thus the distance between the donor and acceptor is increased which results in the FAM fluorescence enhancement.

Effect of Ag⁺ Ions on the Fluorescence Emission of P₁. For evaluation of validity of the proposed principle, the effect of different concentrations of Ag⁺ ions on the fluorescence emission of P₁ was first tested in MOPS buffer solution. In the buffer solution without Ag⁺ ions, the free probe emits strong FAM fluorescence, indicating that there is little quenching of FAM by the quencher in the random coil structure. As expected, the fluorescence of P₁ was decreased rapidly with the addition of Ag⁺ ions. In our experiment, more than 96% quenching was observed and the fluorescence was gradually reached stable when the Ag⁺ ions concentration is over 2.5 μM (trace a, Figure 2). To test whether the P₁ fluorescence decrease is due to the direct fluorescence quenching of FAM by Ag⁺ ions, effect of Ag⁺ ions on the P₃ fluorescence was investigated under the same condition. As for the reference P₃, the fluorescence was slightly decreased with the increment of Ag⁺ concentration from 0 to 10 μM (trace b, Figure 2). These results indicate that silver-mediated base pairs of P₁ are formed between cytosine

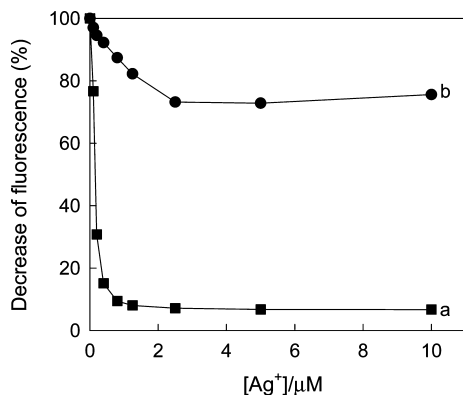


Figure 2. Fluorescence decrease of P_1 (50 nM, trace a) and P_3 (50 nM, trace b) as a function of Ag^+ concentration in MOPS buffer solution (10 mM, pH 7.0, 100 mM Na^+ , 2.5 mM Mg^{2+}). Fluorescence intensity was recorded at 518 nm with an excitation wavelength of 480 nm.

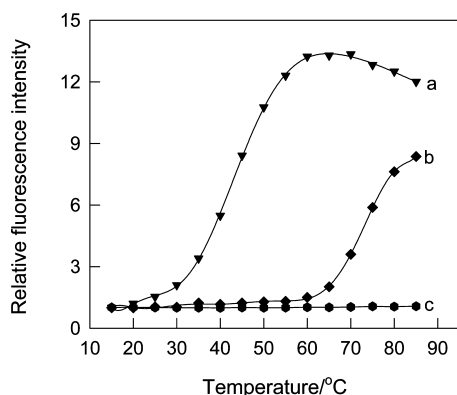


Figure 3. Normalized fluorescence intensity of P_1 (50 nM) in the MOPS buffer solution as a function of temperature with different Ag^+ concentrations: a, 0.1; b, 1.0; and c, 10 μM . For comparison, fluorescence enhancements were normalized to that at 15 $^{\circ}C$. Fluorescence emission was recorded at 518 nm with an excitation wavelength of 480 nm.

residues to form a stable hairpin structure, which leads to an enhanced FRET process between the FAM and Dabcyl moieties.³⁹

Tuning Stem Stability by Ag^+ Ions Ligations. The dependence of the P_1 fluorescence quenching efficiency on the Ag^+ concentration indicates that in the presence of Ag^+ ions, P_1 forms a hairpin-shaped structure with the metal ion (P_1-Ag). Therefore, the stem stability of P_1 was investigated by measuring the melting temperature (T_m) in the presence of different concentrations of Ag^+ ions. T_m was defined as the temperature at which the fluorescence reaches 50% of its maximum value. In the absence of Ag^+ ions, P_1 showed no melting transition between 15 and 85 $^{\circ}C$, because the probe was single stranded DNA in a random coil structure (data not shown). Figure 3 shows the fluorescence emission enhancement of P_1 as a function of temperature, the fluorescence was normalized for convenience between the minimum and maximum fluorescence intensity. Fixing the concentration of P_1 at 50 nM, when Ag^+ ions concentration was changed from 0.1 to 1.0 μM , the T_m of P_1 was increased from 45 to 76 $^{\circ}C$, which is comparable or higher than thermal stability of regular MBs. When the Ag^+ concentration was 5 μM , P_1 was found to be stable at high

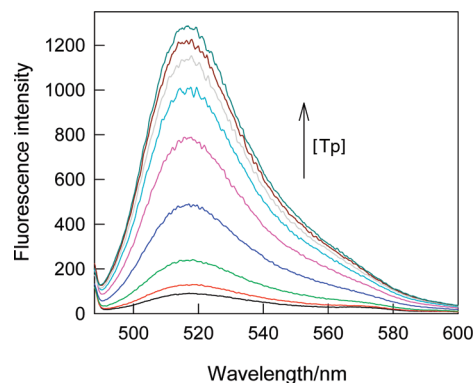


Figure 4. Fluorescence emission spectra of P_1-Ag in the MOPS buffer solution in the presence of different concentrations of target DNA. The arrows indicate the signal changes as increases in the T_p concentration (0, 1.0, 2.0, 5.0, 10, 20, 40, 50, and 80 nM). Each spectrum was recorded with an excitation wavelength of 480 nm after stirring for 1 min upon the target DNA addition. The concentrations of P_1 and Ag^+ ions were 50 nM and 0.5 μM , respectively.

temperatures, even at 85 $^{\circ}C$. These results support the stem stability of P_1 depended on the Ag^+ ions concentrations, which in turn, provides the basis for the design of conformational DNA switch that works well at different temperatures by independently changing the Ag^+ ions concentration.

DNA Hybridization Assay with P_1-Ag . Take together, these findings demonstrate that conformational DNA switches of P_1 based on the Ag^+ ions ligation could be an alternative approach for use in probing DNA hybridization. We thus successively evaluated the capability of P_1-Ag for detection of T_p . It is worth noting that, in the absence of Ag^+ ions, the fluorescence of P_1 was slightly affected by its perfectly complementary target T_p due to the conformational alternation of P_1 from a random coil structure to a duplex. On the contrary, if P_1 was first interacted with Ag^+ ions and subsequent introduction of the same amount of T_p to the P_1-Ag complex solution, P_1-Ag exhibits obvious fluorescence restoration, which presents up to a 11-fold enhancement of fluorescence after the addition of 50 nM T_p (see below). This result indicate that the binding of target DNA by the loop sequence of P_1 unfolds the C- Ag^+ -C structure through formation of a duplex, and constitutes the basis for fluorescent assay of DNA hybridization using this design.

Figure 4 shows the quantitative detection of DNA by using P_1-Ag upon introducing different concentrations of T_p . Upon the addition of an increasing amount of T_p , there is a dynamic increase in the P_1 fluorescence signal. When the target DNA concentration was about 100 nM, the fluorescence intensity of P_1 gradually leveled off with a 14-fold enhancement. Higher DNA concentration produced only small intensity variation. Trace c of Figure 5 shows the P_1 fluorescence enhancement as a function of the T_p concentration, a linear relationship was observed with a region from 1.0 to 50 nM T_p .

An important feature of P_1-Ag is that the DNA assay characteristic, such as detection sensitivity, hybridization dynamics, and the selectivity, can be modulated by adjusting the concentrations of Ag^+ ions because the stem stability is determined by the Ag^+ concentration. The amount of complexed Ag^+ ions in the system influences blank fluorescence intensity of P_1 , and thus its response range for its target DNA.

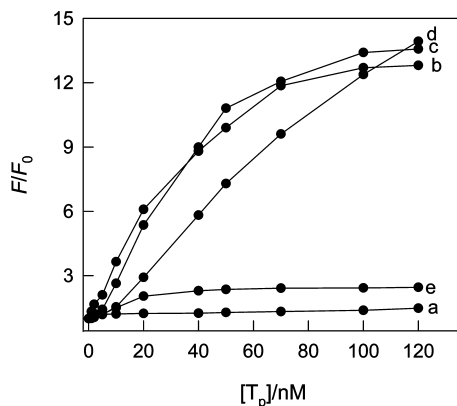


Figure 5. Relative fluorescence intensity of P_1 in the MOPS buffer solution as a function of different concentrations of target T_p with varying the Ag^+ ions amounts (from trace a to trace e: 0, 0.2, 0.5, 1.0, and 2.0 μM). F and F_0 are the fluorescence intensity of P_1 in the absence and in the presence of target DNA, respectively.

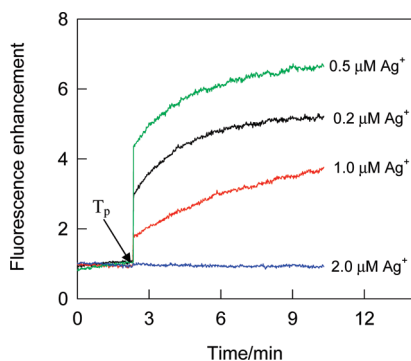


Figure 6. Real-time fluorescence records of P_1 (50 nM) with different concentrations of Ag^+ (0.2, 0.5, 1.0, and 2.0 μM) upon addition of 20 nM target T_p , respectively. For comparison, fluorescence enhancements were normalized to that in the absence of T_p at all cases. Fluorescence emission was recorded at 518 nm with an excitation wavelength of 480 nm. The transition between each regime is marked with an arrow.

Lower concentrations of Ag^+ ions result in the higher background fluorescence, and thus decrease the sensitivity and response range of the measurement. However, the amount of Ag^+ in the system should not be too high. Otherwise, the stem portion could not be opened even if high concentration of target was added. Fixing the concentration of P_1 at 50 nM, Figure 5 shows the fluorescence enhancement of P_1 in the presence of different concentrations of Ag^+ as functions of T_p concentrations. With Ag^+ concentration of 0.2 μM , the best detection range was from 1.0 to 40 nM, while the Ag^+ concentration was increased to 0.5 μM , the detection range was extended from 10 to 100 nM. The flexibility of Ag^+ ions controlling allows us to monitor the DNA concentration with appropriate adjustment of the metal concentration, so that the sample response falls within the most sensitive region.⁵⁴

The DNA hybridization kinetics of P_1 could be modulated by different amounts of Ag^+ ions. Figure 6 shows the real-time fluorescence records of P_1 upon additions of Ag^+ ions and subsequent target T_p . Low Ag^+ concentration caused rapid

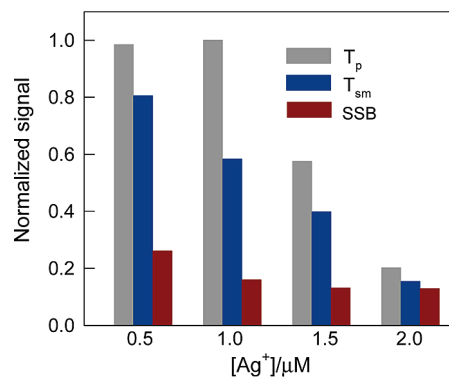


Figure 7. Fluorescence changes of P_1 (50 nM) in MOPS buffer solution in the presence of T_p , T_{sm} , and SSB versus Ag^+ ions concentrations. The concentrations of targets were 50 nM, respectively. Fluorescence signal enhancements were normalized to the maximal T_p signal when 1.0 μM Ag^+ was used.

kinetic response, increases in Ag^+ concentration reduced DNA hybridization rate, but with decreased background fluorescence. From Figure 6 one can see that, the stable readout time in the Ag^+ ion concentration range for DNA hybridization was 5–10 min, which is shorter than that of T-Hg²⁺-T - based MBs,^{44,45} but is slightly longer than that of conventional MBs based on Watson–Crick-based duplex. The slow hybridization kinetics could be explained by the high energy barrier created by the necessity of destroying the C– Ag^+ –C structures. The phenomenon is similar to the slow binding kinetics observed for MBs with a long stem. Overall, therefore, this flexibility of DNA binding kinetics allows us to formulate a novel DNA hybridization assay system suitable for the particular requirement of a given analytical method, and is one of the advantages that the proposed approach has over regular MBs.^{31,52}

A significant advantage of MBs stems from the high degree of specificity with which they can recognize target sequences. But we expect that the flexibility of the stem formed by C– Ag^+ –C will make P_1 – Ag outperform conventional MBs in view of its operation convenience and high power to discriminate between the perfect target and the mismatches. Two kinds of target DNA sequences including the complementary target DNA (T_p) and the single base-mismatch DNA (T_{sm}) were chosen to study the selectivity. We thus measured the signal difference between T_p and T_{sm} in the solution with different concentrations of Ag^+ ions. Figure 7 shows the comparison of the P_1 fluorescence enhancement induced by T_p and T_{sm} in the presence different amounts of Ag^+ ions. From Figure 7 one can see that, P_1 containing 1.0 μM Ag^+ was able to give a better mismatch discrimination of a single base-difference. At this Ag^+ concen-

- (55) Tang, Z. W.; Mallikaratchy, P.; Yang, R. H.; Kim, Y.; Zhu, Z.; Wang, H.; Tan, W. H. *J. Am. Chem. Soc.* **2008**, *130*, 11268–11269.
- (56) Tang, Z. W.; Zhu, Z.; Mallikaratchy, P.; Yang, R. H.; Sefah, K.; Tan, W. H. *Chem.–Asian J.* **2010**, *5*, 783–786.
- (57) Jhaveri, S. D.; Kirby, R.; Conrad, R.; Maglott, E. J.; Bowser, M.; Kennedy, R. T.; Glick, G.; Ellington, A. D. *J. Am. Chem. Soc.* **2000**, *122*, 2469–2473.
- (58) Nutiu, R.; Li, Y. *J. Am. Chem. Soc.* **2003**, *125*, 4771–4778.
- (59) Merino, E. J.; Weeks, K. M. *J. Am. Chem. Soc.* **2003**, *125*, 12370–12371.
- (60) Wang, J.; Jiang, Y. X.; Zhou, C. S.; Fang, X. H. *Anal. Chem.* **2005**, *77*, 3542–3546.
- (61) Sazani, P. L.; Larralde, R.; Szostak, J. W. *J. Am. Chem. Soc.* **2004**, *126*, 8370–8371.
- (62) Zuo, X. L.; Song, S. P.; Zhang, J.; Pan, D.; Wang, L. H.; Fan, C. H. *J. Am. Chem. Soc.* **2007**, *129*, 1042–1043.

(54) Liu, J. W.; Lu, Y. *J. Am. Chem. Soc.* **2003**, *125*, 6642–6643.

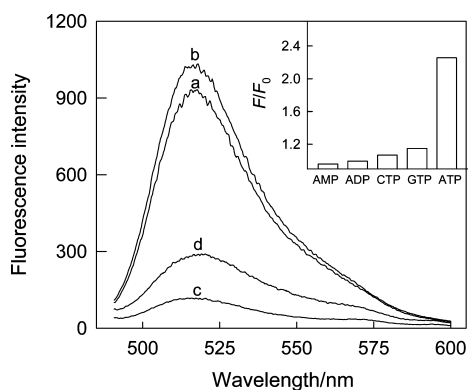


Figure 8. Fluorescence emission spectra of P_2 (50 nM, $\lambda_{\text{ex}} = 480$ nm) under different experimental conditions: (a), P_2 in MOPS buffer solution; (b), (a) + 1.0 mM ATP; (c), (a) + 0.5 μM Ag^+ ions; and (d), (c) + 1.0 mM ATP. Inset: fluorescence changes of $P_2\text{-Ag}$ (0.5 μM Ag^+) in MOPS buffer solution induced by different targets (1.0 mM, x-axis markers) under the same conditions.

tration, the fluorescence enhancement of P_1 induced by 50 nM P_{sm} is about 58% that by T_p under the same conditions. Higher Ag^+ concentration reduced the capability of SNPs, because the $\text{C-Ag}^+\text{-C}$ structures are too strong to be unfolded by T_p . To further study the target DNA binding specificity, we investigated the resistance of the P_1 toward nonspecific binding protein using single-stranded binding protein (SSB). This is necessary because the conventional MBs are subject to nonspecific binding to SSB, which give false positive signals. In the assay, if the P_1 binds to SSB, the fluorescence will increase because the fluorophore will separate from the quencher. As shown in Figure 7, the fluorescence enhancement of induced P_1 by SSB was significantly smaller than that by target DNA under the same conditions. The results suggest that the P_1 could improve the ability to resist nonspecific binding, which makes this probe well suited to monitor a substrate in the complex biological milieu containing nonspecific binding substrates.

Detection of ATP with P_2 . To demonstrate the versatility of this design, we used the same principle and molecular scheme to design and synthesize a nucleic acid probe (P_2 , Table 1) targeting a small molecule, ATP. The probe sequences is similar to that of our previous design,^{55,56} which is composed of an aptamer for ATP, a short DNA sequence complementary to part of the aptamer and a poly T linker connecting these two. A fluorophore and a quencher are covalently attached at the two terminus of the conjugated DNA sequences, but it could not form an intramolecular fluorescence-quenching approach, because the labeled fluorophore and quencher are of space separation. Figure 8 shows the fluorescence emission spectra of P_2 at different conditions. Spectrum a was measured in the buffer solution in the absence of Ag^+ ions, where P_2 shows strong FAM fluorescence. Addition of 1.0 mM ATP to the solution induced a few enhancement of the FAM fluorescence emission (spectrum b), indicating that the target binding hardly changed the molecule conformation of P_2 . In the presence of Ag^+ ions in the solution of P_2 , the fluorescence emission by FAM was greatly decreased, which is ca. 0.12-fold that of the free P_2

(spectrum c), suggesting the formation of a conformationally constrained structure, bringing a fluorophore and a quencher into close proximity. Spectrum d of Figure 8 shows the fluorescence emission spectrum of $P_2\text{-Ag}$ in the presence of 1.0 mM ATP. Binding of the aptamer with ATP leads to obvious restoration of the FAM emission. In Figure 8, the ratio of F/F_0 of P_2 in the presence of 1.0 mM ATP was estimated to be 1.08, while the value of $P_2\text{-Ag}$ went up to 2.3 upon the addition of same concentration of ATP. The limit detection, based on 3 times the signal-to-noise level, was estimated to be 0.2 mM, which is comparable with that of the regular dye-quencher pair-labeled aptamers.^{57–59} These results indicate that the formation of conformationally constrained form makes P_2 be efficient in probing small molecule binding. To understand the response behaviors of P_2 toward different targets, the fluorescence intensity changes of $P_2\text{-Ag}$ by structural similar molecules (AMP, ADP, CTP, and GTP) were studied (inset of Figure 8). No obvious fluorescence change could be observed by AMP, ADP or CTP. But when tested with GTP at the concentration of 1.0 mM, $P_2\text{-Ag}$ produced a slight fluorescence enhancement. The selectivity of $P_2\text{-Ag}$ is similar to the original ATP aptamers,^{60–62} confirming that the design does not affect the selectivity of the aptamer.

CONCLUSION

The success of the Ag^+ complexes of P_1 and P_2 for detections of nucleic acid and small molecule unquestionably supports the feasibility that the construction of conformationally constrained DNA probes could be easy achieved by using specific metal-ligation interaction. With regard to the traditionally used stem-containing probes based on a Watson–Crick duplex, the central hallmark of the design is the feasibility to conveniently tune the stem-stability by simple alteration of the metal ions concentration, and thus kinetic and thermodynamic characteristic of the probes. In addition, due to the higher affinity of metal-ligation over Watson–Crick hydrogen bonds, these metal-modulated conformationally constrained probes are suitable to applications in complex biological environments. Finally, compared to the analogue designs based on $\text{K}^+\text{-G}$ -quadruplex and $\text{T-Hg}^{2+}\text{-T}$ structures, the present approach possesses tunable and strong conformation stability but without lengthy protocols, sophisticated probe design, and the use of toxic Hg^{2+} ions. These features establish the simplicity, effectivity and universality of the platform and could, therefore, provide the groundwork for the design of function nucleic acid probes for biosensing applications.

ACKNOWLEDGMENT

The work was supported by the National Natural Science Foundation of China (20775005) and the National Grand Program on Key Infectious Disease (2009ZX10004-312).

Received for review April 28, 2010. Accepted June 23, 2010.

AC101114W